THE UNIVERSITY OF NEW MEXICO

CQuIC Center for Quantum Information and Control

SAND2020-1930PE

Neutral Atom Projects for Improvements in Quantum Metrology and Information

PRESENTED BY

John Bainbridge

Sandia National Laboratories is a multimission laboratory managed and operated by National Technology & Engineering Solutions of Sandia, LLC, a wholly owned subsidiary of Honeywell International Inc., for the U.S. Department of Energy's National Nuclear Security Administration under contract DE-NA0003525.

Organizational Overview

Part 1: Work on the Rydberg project

I. Introduction to the Rydberg project

II. Design and characterization of a microwave resonator

III. Characterization of the high NA trapping/imaging system

Part 2: Work on an Atomic Magnetometer for RF Field detection

I. Introduction our optically pumped magnetometer (OPM)

II. Modeling and the master equation

III. Results

IV. Future work

Part 3: Acknowledgements

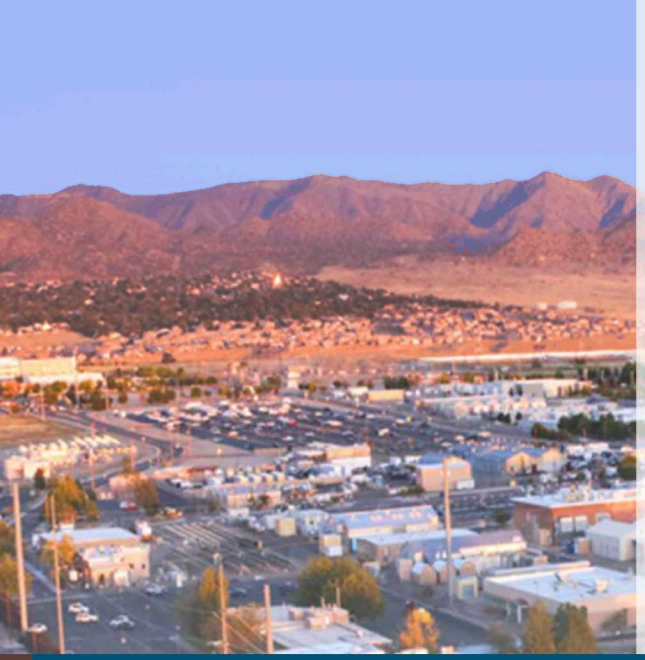

Part 1-I:Introduction to the Rydberg project

Neutral Atom Qubits: Pros and Cons

Pros

1. Long trap lifetimes[1,2].
2. Minimal effects on other atoms.
3. Can be arranged (and re-arranged!) into arbitrary arrays of >100 atoms[2,3,4,6].
4. Very useful for metrology
   - Atom interferometers.
   - DC electric fields.
   - Optical clocks.

Entangled states can be used to exceed standard quantum limit (SQL)!

Cons

1. Difficult to entangle with high fidelity, but getting there.
   - Best demonstrated fidelity at Sandia was (~0.89), has now been matched by others.[5,7]
   - Harvard group has achieved fidelity of >0.97!

(1) A.M HANKIN, "*RYDBERG EXCITATION OF SINGLE ATOMS FOR APPLICATIONS IN QUANTUM INFORMATION AND METROLOGY,*". PH.D THESIS, 2015.
(2) A. COOPER ET AL, "*ALKALINE-EARTH ATOMS IN OPTICAL TWEEZERS*," PHYSICAL REVIEW X **8**, 041055(2018).
(3) M. ENDRES ET AL, "*ATOM-BY-ATOM ASSEMBLY OF DEFECT FREE ONE-DIMENSIONAL COLD ATOM ARRAYS*," SCIENCE *VOL.* 354, 2016.
(4) F. NOGRETTE ET AL. "*SINGLE-ATOM TRAPPING IN HOLOGRAPHIC 2D ARRAYS OF MICROTRAPS WITH ARBITRARY GEOMETRIES*," PHYSICAL REVIEW X **4,** 021034, 2014.
(5) G.W. BIEDERMANN AND M.J. MARTIN "CPHASE GATE WITH RYDBERG ATOMS (CPHAR)" SANDIA REPORT SAND2017-12802.
(6) M.J. MARTIN, M.C. REVELLE, AND G.W. BIEDERMANN, "*A PLATFORM FOR QUANTUM INFORMATION AND LARGE-SCALE ENTANGLEMENT WITH RYDBERG ATOMS IN PROGRAMMABLE OPTICAL POTENTIALS*", SANDIA REPORT SAND2019-1030, AVAILABLE ONLINE AT HTTPS://WWW.OSTI.GOV/SERVLETS/PURL/1493463.
(7) C.J. PICKEN ET AL. "*ENTANGLEMENT OF NEUTRAL-ATOM QUBITS WITH LONG GROUND-RYDBERG COHERENCE TIMES*," QUANTUM SCI. TECHOL. **4,** 015011, 2018.
(8) H. LEVINE ET AL. "HIGH-FIDELITY CONTROL AND ENTANGLEMENT OF RYDBERG-ATOM QUBITS" , PRL 121, 123603 (2018)

Example Trap Arrays

Below: 3D trap arrays generated by D. Barredo et al. at the Institut d'Optique.

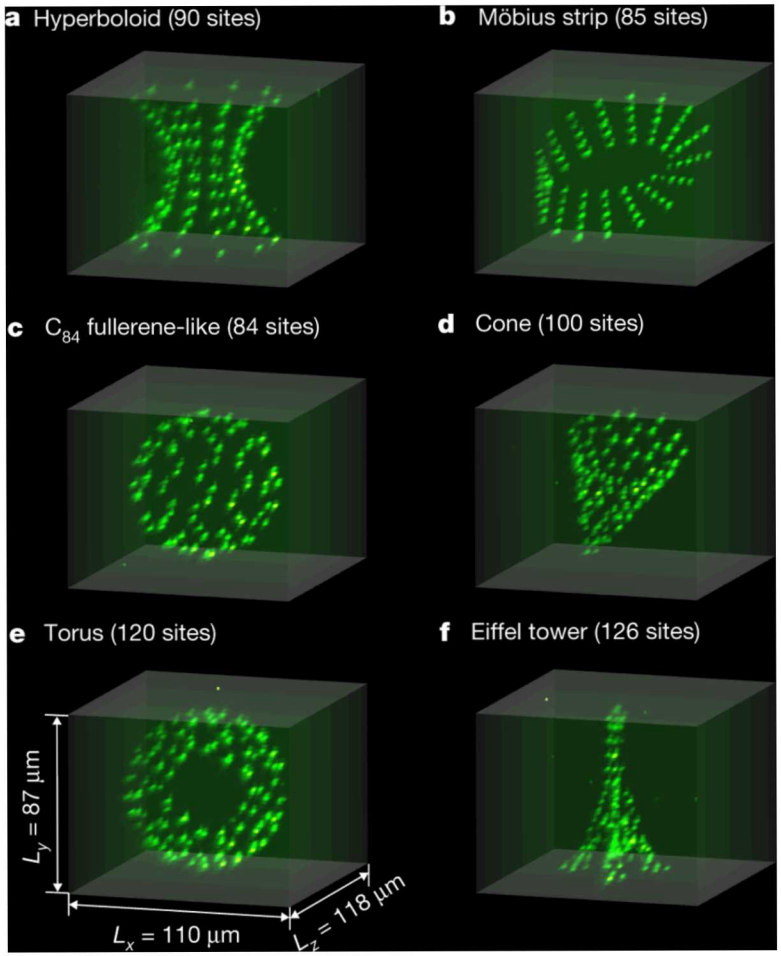

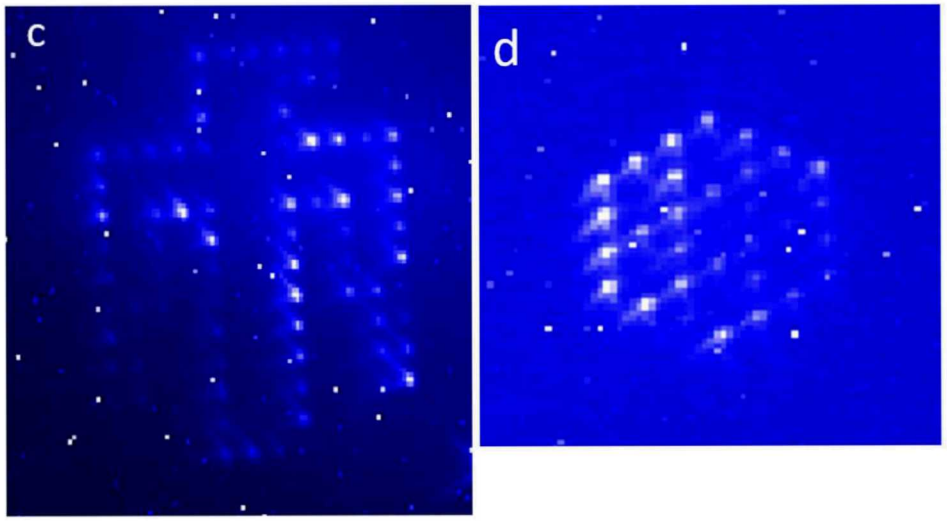

Above: 2D trap arrays generated by M. Revelle and M. Martin at Sandia.

It's relatively easy to make arrays of >100 trap sites with neutral atoms!

Neutral Atom Entanglement: Rydberg States

Need to execute an *entangling* gate. Neutral atoms make this challenging.

- Most promising approach: use Rydberg states! Sandia has a single photon laser at 318 nm to excite the $6S_{1/2} \rightarrow 64P_{3/2}$ transition.[1]
- Characteristic size of the position space wavefunction scales as $\langle r \rangle \propto n^2$ so the atom grows by $58^2 = 3364$! The dipole operator $\hat{\boldsymbol{P}} = q\hat{\boldsymbol{r}}$ scales the same way.
- With this large dipole moment, the dipole-dipole interaction $\hat{\boldsymbol{H}} = -\hat{\boldsymbol{P}}_1 \cdot \hat{\boldsymbol{P}}_2$ can provide an entangling gate.
  - Atoms are brought close together ($r < 1\ \mu m$) to compensate the $1/r^6$ scaling.

(1) A.M HANKIN, "RYDBERG EXCITATION OF SINGLE ATOMS FOR APPLICATIONS IN QUANTUM INFORMATION AND METROLOGY,". PH.D THESIS, 2015.

Neutral Atom Entanglement: The Rydberg Blockade

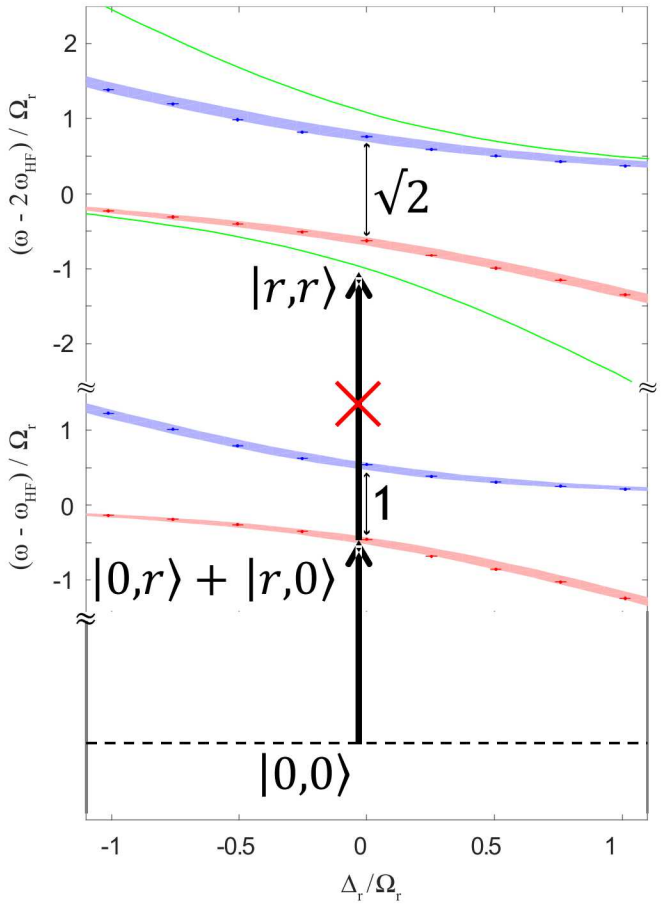

1. Large dipole-dipole interaction causes a light shift ΔE_{LS} between the $|F = 4, m_F\rangle$ ground state and the Rydberg state $|r\rangle$.
2. $|F = 4, m_f\rangle \leftrightarrow |r\rangle$ shifts *out* of resonance with the 318 nm laser for the other atom.
3. Thus we have a single *collective* excitation into the Rydberg state.

We use this to employ "Rydberg dressing". It works by detuning the Rydberg laser to create a superposition $|\psi\rangle = a|1\rangle + b|r\rangle$ with small b to avoid dephasing.

Figure from Y.-Y. Jau et al, "Entangling Atomic Spins with a Strong Rydberg Dressed Interaction", *Nature Physics*. 12 (71-74), (2016).

Part 1-II: Design and Characterization of a Microwave Resonator

Single Photon Control?

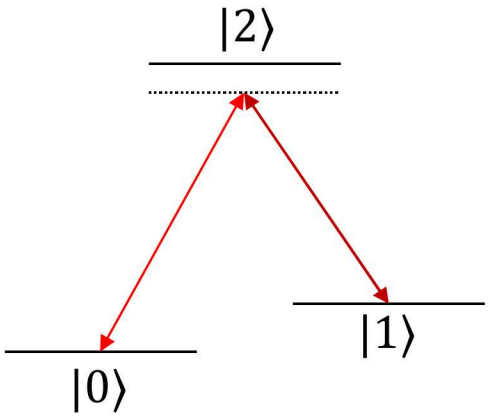

?

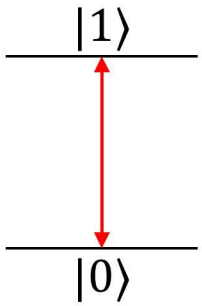

Pros

1. No off resonant scattering.
2. No need to worry about relative phase.
3. High stability.

Cons

1. Slow.
2. Harder to implement.
3. No momentum kick for interferometry.

A Resonant Structure for Microwave and DC Field Control?

Can the current Faraday cage be modified to a*lso* be a microwave resonator? To work, the design must:

1. Resonate at the Hyperfine "clock" frequency of ^{133}Cs.
2. Have correct polarization(π polarized- magnetic field).
3. Maintain full optical access.

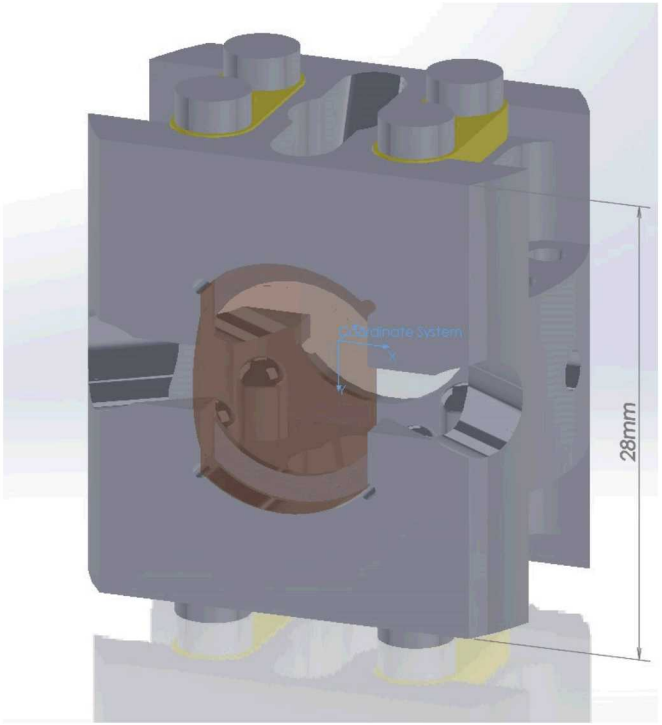

Above: CAD model of the current design of the Faraday cage used for DC field control.

A Candidate Solution: The $TE_{1,2,0}$ Mode of a Rectangular Resonator

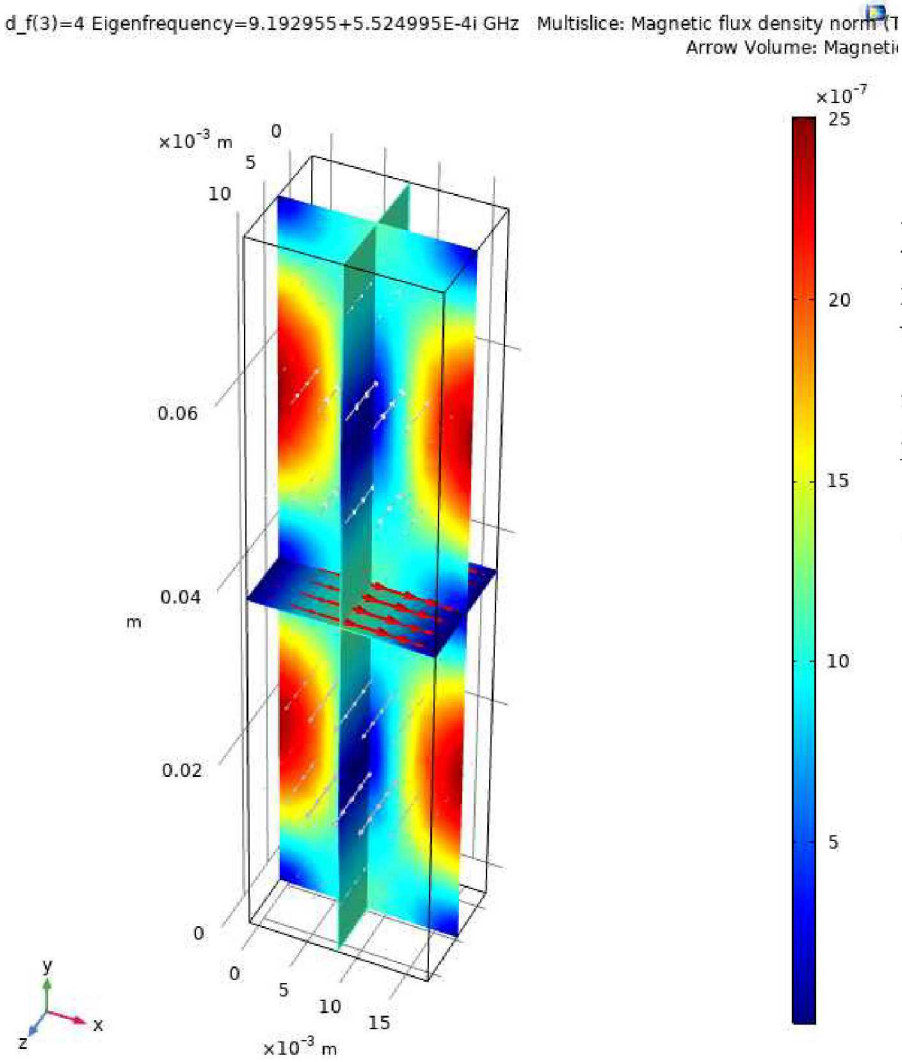

Left: Magnetic field of the $TE_{1,2,0}$ mode of a rectangular resonator.* White arrows are electric field and red arrows are magnetic field. Color legend in T.

.

*Simulation of the resonant field distribution generated using *COMSOL Multiphysics*, the same package used for field simulations of the prototype.

Faraday Resonator Prototype

- Prototype designed Using *SolidWorks* for CAD design and *COMSOL Multiphysics* for finite element method (FEM) simulations.
- There are several major challenges in properly simulating the design:

1. How to handle open boundaries when approximating solutions to Maxwell's equations?
2. How to properly couple in the microwaves?

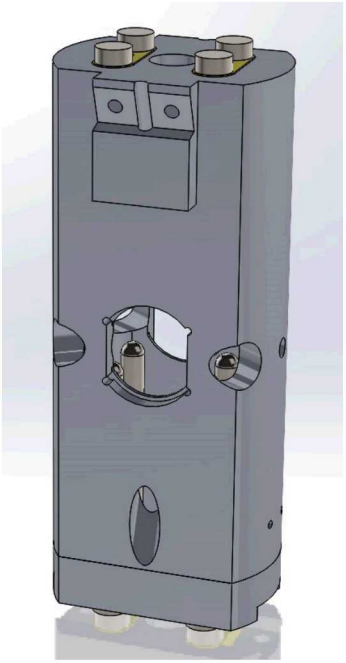

Left: The CAD model of the prototype

Right: An image of the fabricated prototype

Coupling in the Field: A Game of Modes

Coupling in the field is a matter of mode-matching the antenna to the cavity.

Current design is a single antenna made by striping the end of a coaxial.

Antenna inserted from one side at a 20° angle.

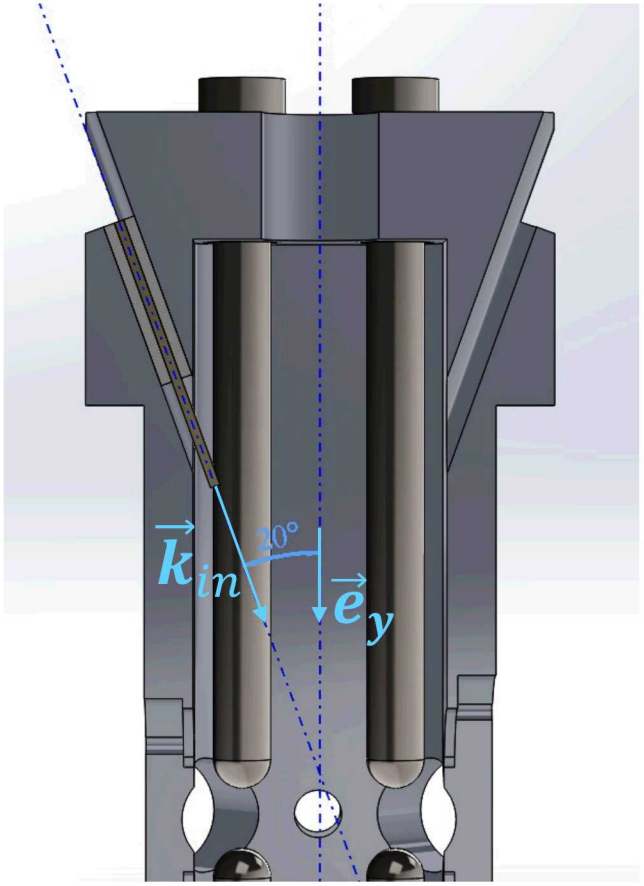

Above: Cutaway view showing the antenna input

Experimental Response of the Prototype

(a)

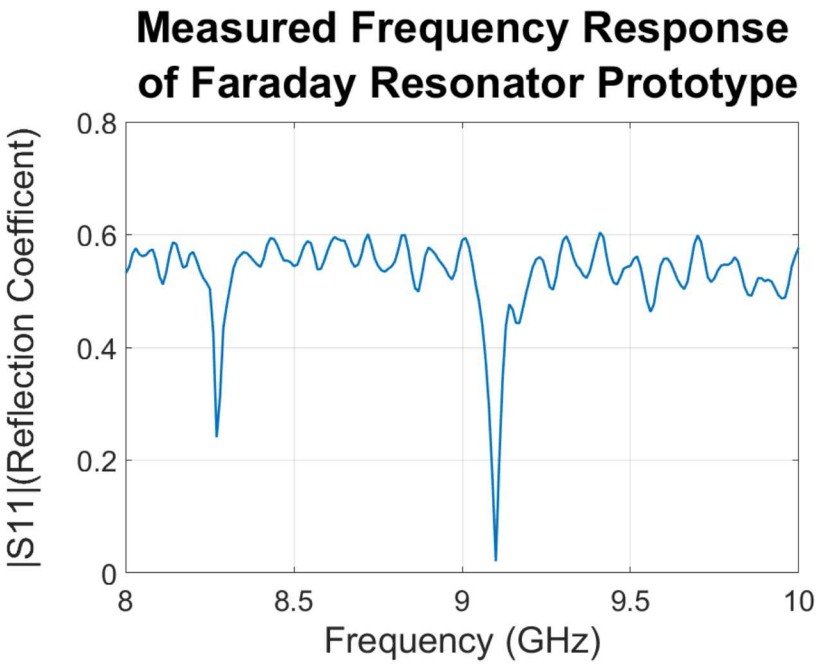

(b)

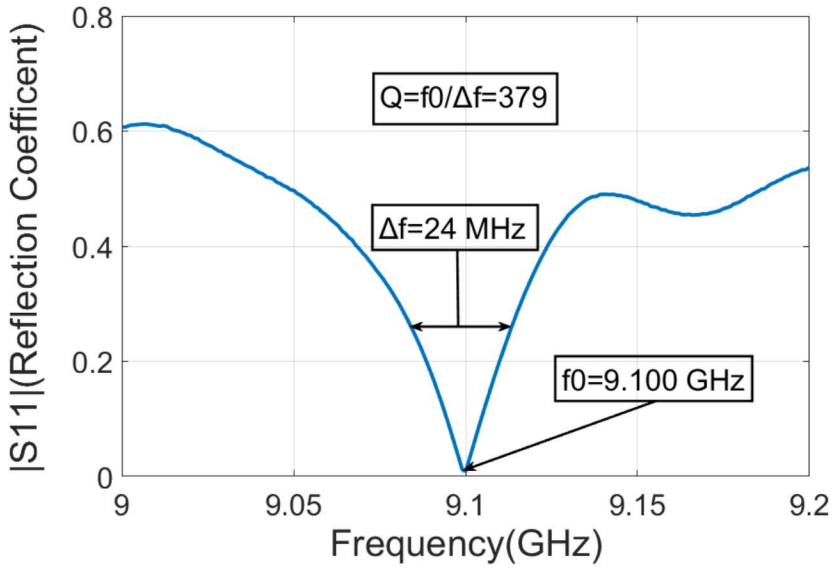

Above: (a) The Frequency response of the prototype. Maximum (critical) coupling is achieved when $|S_{11}| = 0$. **(b)** A closeup of the resonance of interest.

Part 1-III: Characterization of the Trapping/Imaging System

Single Atom Dipole Traps: High NA Imaging

Want $w_0 \leq 1\ \mu m$. A high numerical aperture (NA) imaging system is necessary. For a trapping laser at $\lambda = 938\ nm$

$$NA \geq 0.29.$$

Required for an *ideal* Gaussian trap. Better approximations show

$$NA \geq 0.5.$$

Required in practice.

Moral of the story: Very high NA trap required to achieve a sub-micron trap!

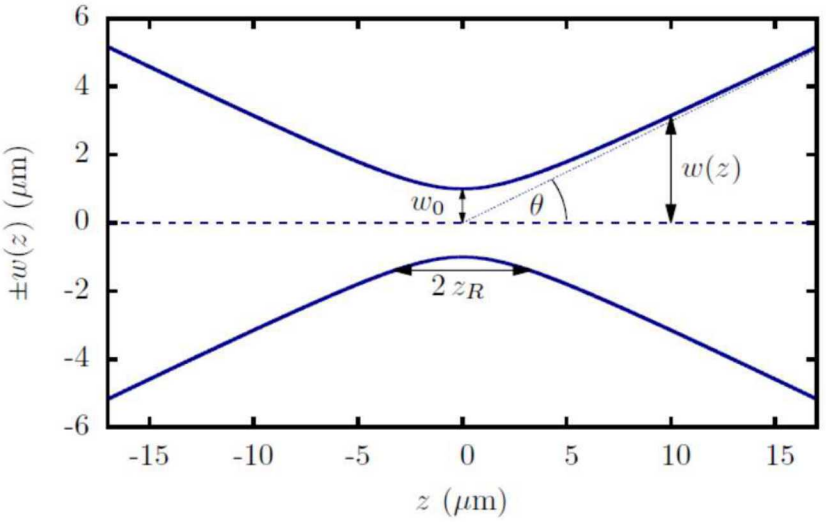

Above: The behavior of a Gaussian beam at it's focus(waist).

Figure from Hankin.

Questions About the Lens

- Currently use a commercial lens (Lightpath Technologies code 355561) designed at the Institut d'Optique.[1]
  - Nominal NA of 0.6.
- Lens designed for ^{87}Rb wavelengths. Does it work at ^{133}Cs wavelengths?
- Measured size is >1μm admeasured trap frequencies too low.

Why? How sensitive is the lens to input tip/tilt? Input displacement?

(1) THE COMMERCIALLY AVAILABLE LENS HAS THE SAME DESIGN SPECIFICATIONS AS THOSE LAID OUT IN LUCAS BEGUIN. "MEASUREMENT OF THE VAN DER WAALS INTERACTION BETWEEN TWO RYDBERG ATOMS." INSTITUT D'OPTIQUE GRADUATE SCHOOL, 2013. CREDIT TO MIKE MARTIN FOR NOTING THIS FACT.

The Point Spread Function

- Even ideal lenses limited by diffraction.
- Minimum spot size characterized by "point spread function (PSF)."
- Ratio of maximum normalized intensity of the PSF to the maximum normalized intensity of an ideal Airy disc is the *Strehl ratio* S.
  - $S \geq 0.8$ arbitrary threshold for diffraction limited performance.
- How does the PSF respond to tip/tilt?
- How does the PSF respond to translations?

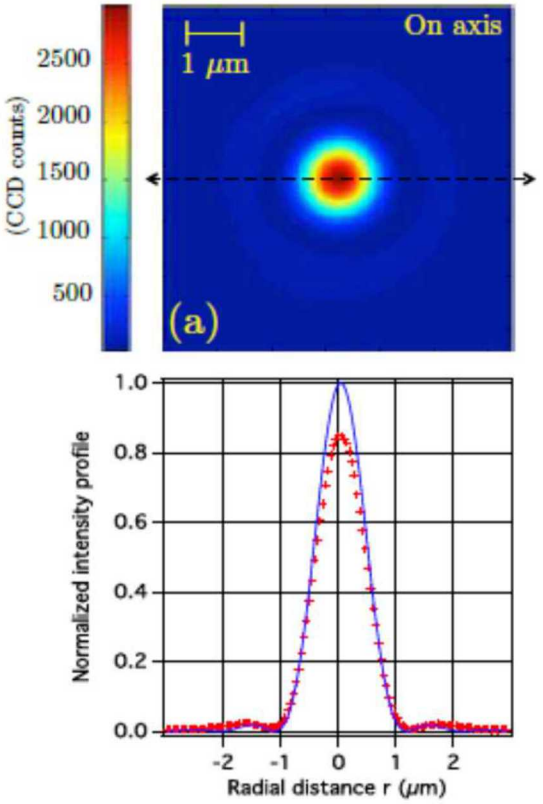

Above: The on axis PSF of the lens at 850 nm as measured at the Institut d'Optique.

Image from the thesis of L. Beguin (2013).

Zemax Results: Soft Dependence on Displacement

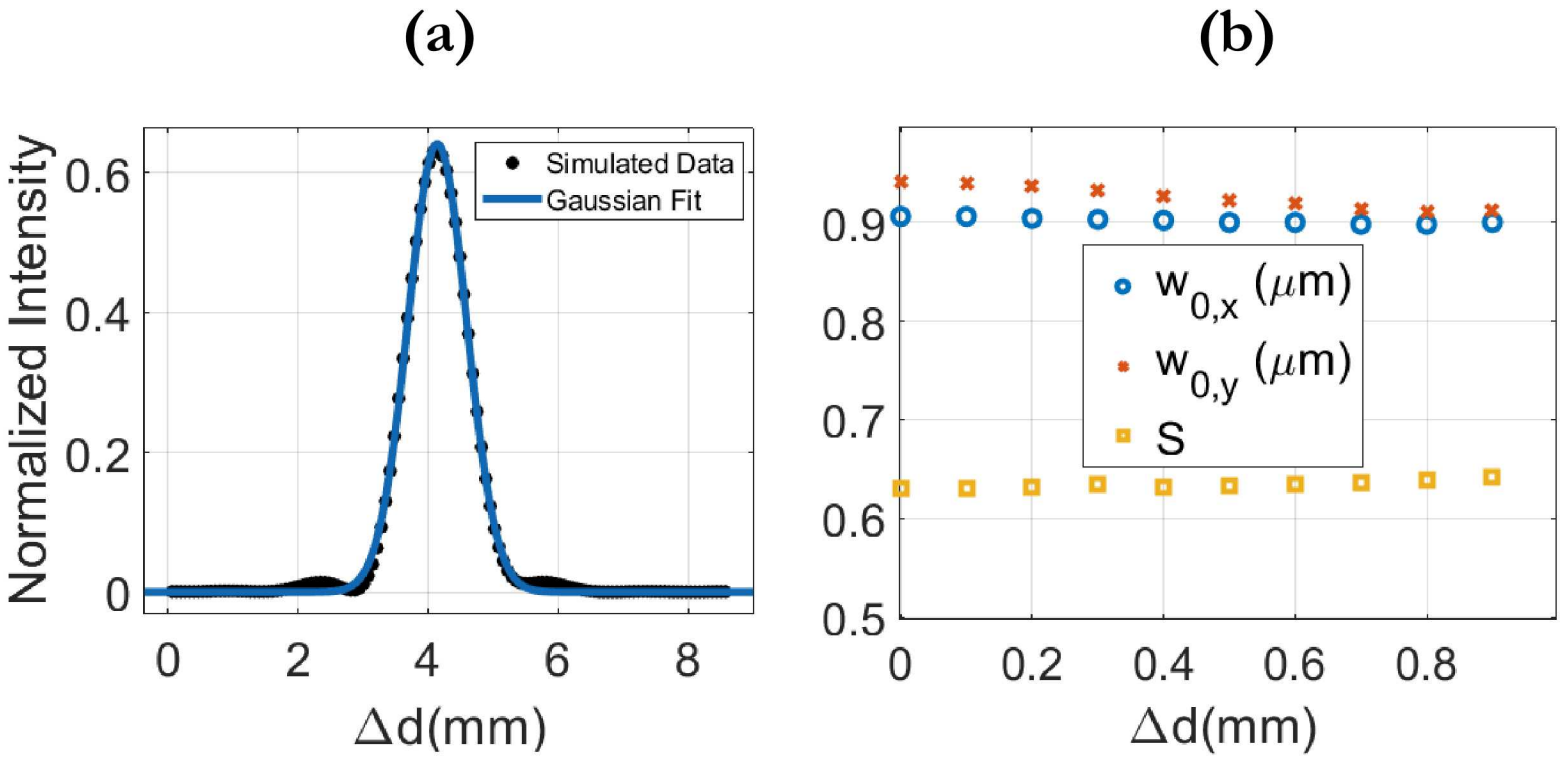

Above: (a) Example of the PSF data generated in *Zemax* for a beam decentered by 500 μm. Gaussian curve fit via *Matlab* to determine the $1/e^2$ size is also shown. **(b)** Behavior of the Strehl ratio and $1/e^2$ size of the beam as a function of beam decentering.

Zemax Results: Stronger Dependence on Angle

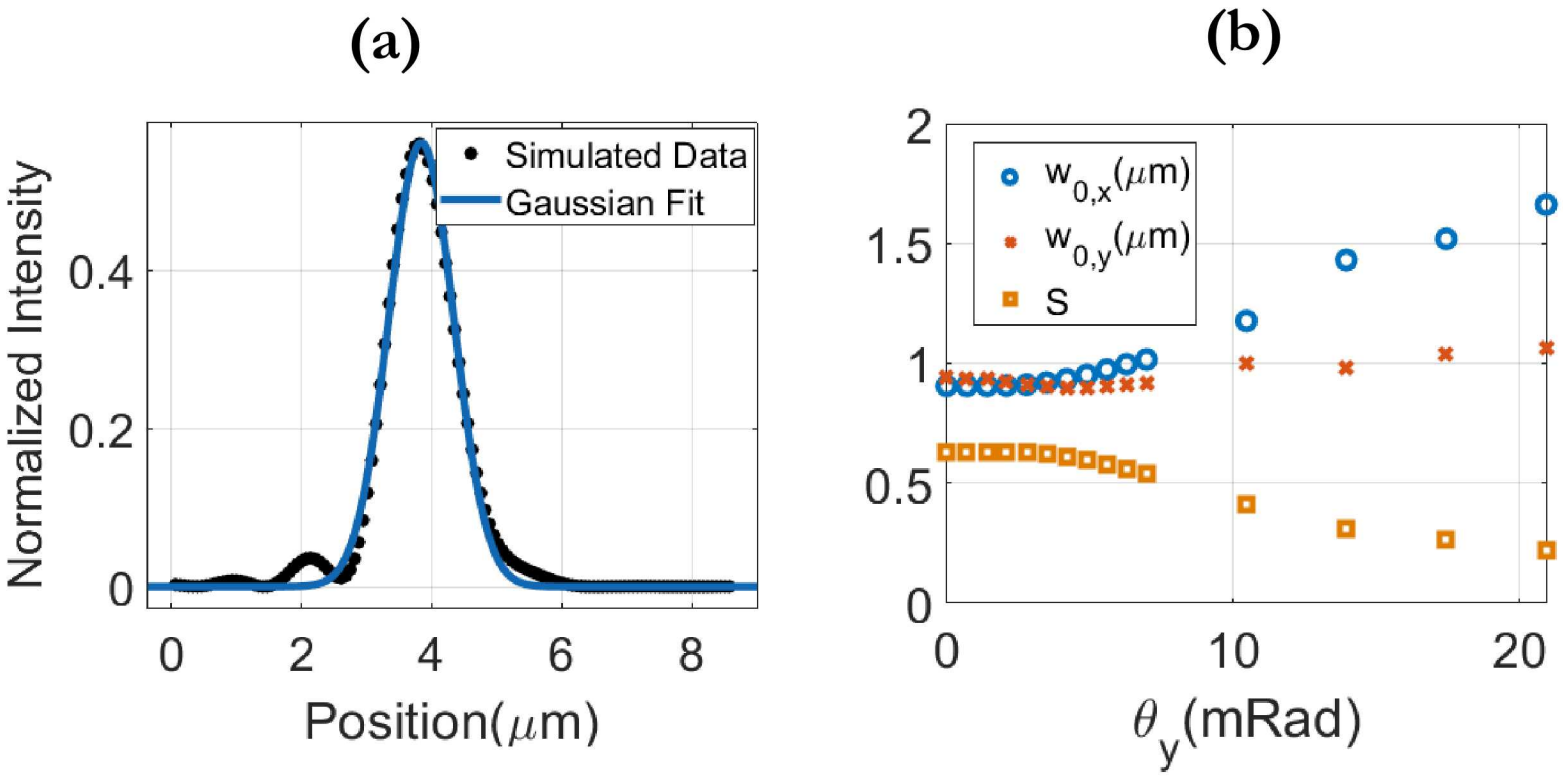

Above: (a) Example of PSF data generated in *Zemax* for a beam that has been tilted by $26.6\ Arcmin = 6.28\ mRad$. The Gaussian curve fit via *Matlab* to determine the $1/e^2$ size is also shown. **(b)** The behavior of the Strehl ratio and $1/e^2$ size of the beam as a function of tilt angle.

Experimental Results

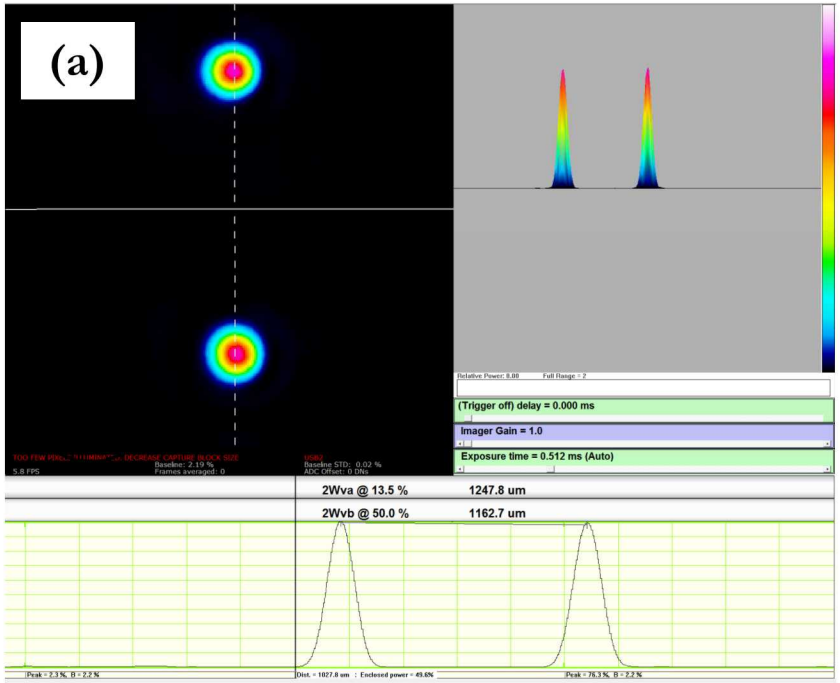

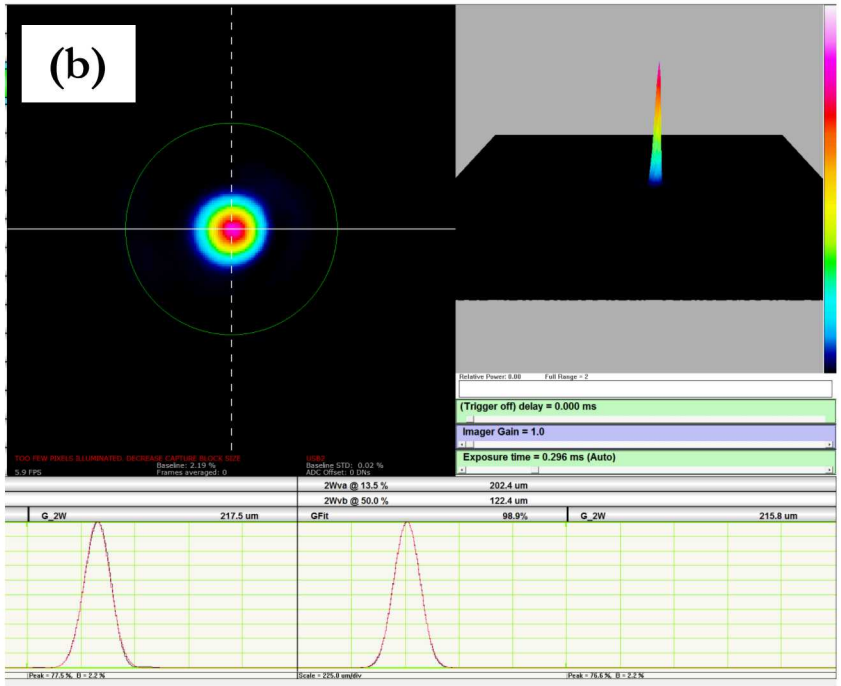

Above: (a) The imaged on-axis point spread function of both trap sites at $\lambda = 938\ nm$. **(b)** The imaged on axis point spread function of the first trap site at $\lambda = 938\ nm$. Both images were captured at a measured magnification of $M = 103.7 \pm 0.28$. Using this along with the pictured fit, the $1/e^2$ radial size of the first trap was found to be $0.98\ \mu m \pm 0.01\ \mu m$.

Comparison of Results

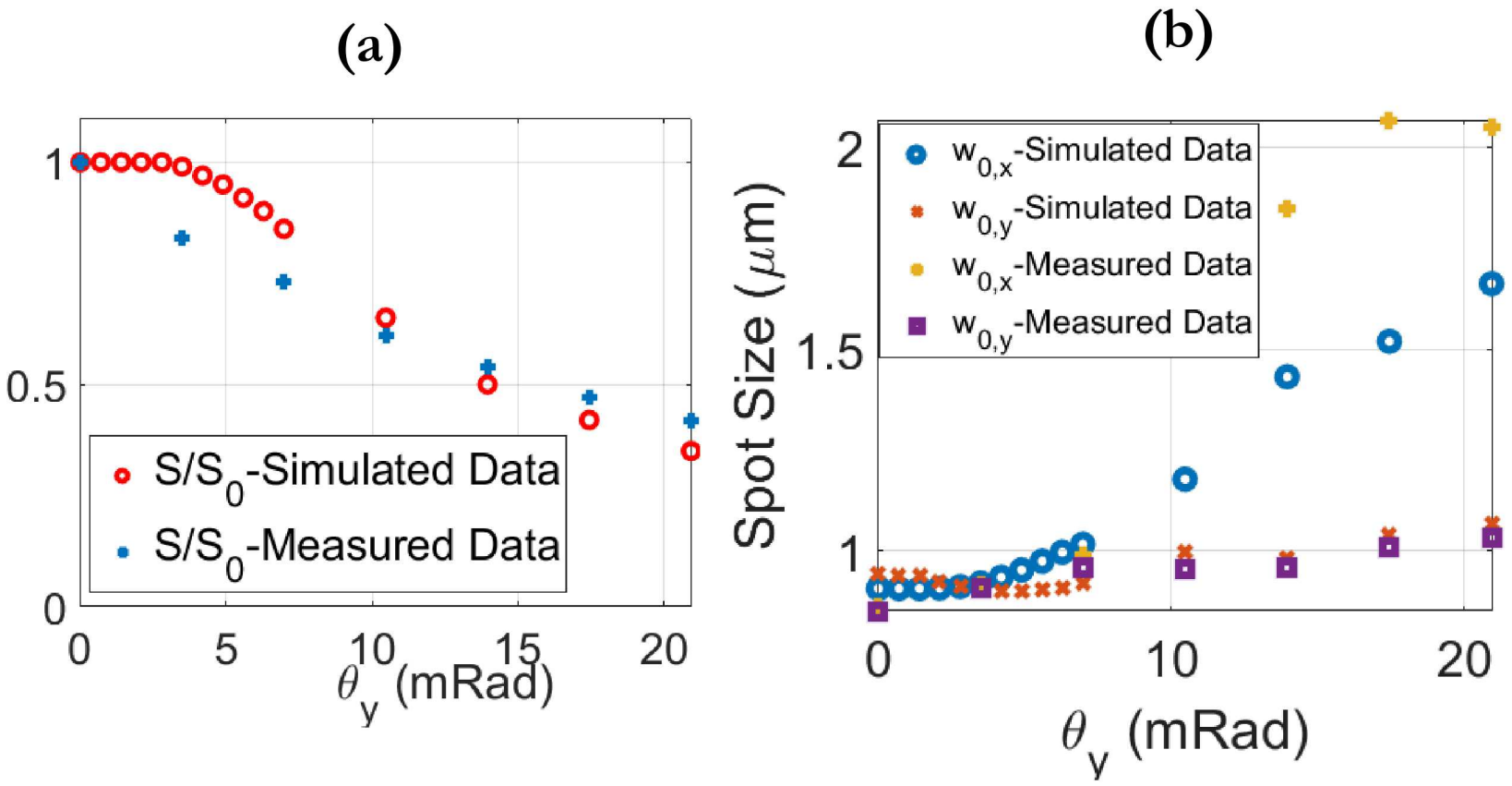

Above: (a) Comparison of simulated Strehl Ratio data to the measured data. **(b)** Comparison of simulated spot size data to measured spot size data.

Conclusions on the Trapping/Imaging System

1. It can achieve sub micron sized traps if perfectly aligned.
2. With $5\ mRad$ available in either direction and $1\ mRad/10\ \mu m$ trap spacing, can achieve a square grid of up to $(5+5)^2 = 100$ trap sites!
3. Achieving the required level of alignment precision is exceptionally difficult.
4. Alternative optical system may be a better option.

Part 2-I:Introduction our Optically Pumped Magnetometer (OPM)

Why Atomic Magnetometers for RF Fields?

1. Can achieve sensitivities $\sim 1 \mathrm{f}T/\sqrt{Hz}$, comparable to superconducting quantum interference devices (SQUIDs) without need for cryogenic cooling.(1)
2. Radio communication with small signal amplitude.
3. Nuclear magnetic resonance (NMR) and nuclear quadrupole resonance(NQR) detection.(2)
4. Fundamental Physics (Axion searches).(3)

(1) Savukov, Seltzer, and Romalis "Tunable Atomic magnetometer for Detection of Radio-Frequency Magnetic Fields". PRL **95**,063004(2005).

(2) Garroway et al. "Remote Sensing by Nuclear Quadrupole Resonance". IEEE Trans. Geosci. Remote Sens. **39**,1108(2001)

(3) Bradley et al. "Microwave Cavity Searches for Dark-Matter Axions". Rev. Mod. Phys. **75**, 777(2003).

Atomic Magnetometers: Larmor Precession

Exploit the Larmor precession of atoms in a magnetic field $\boldsymbol{B} = \mathrm{B}_0\mathbf{e}_z$

$$\omega_0 = \gamma B_0.$$

Where ω_0 is the Larmor precession frequency and γ is the gyromagnetic ratio.

If we know γ, we can measure ω_0 to measure B_0!

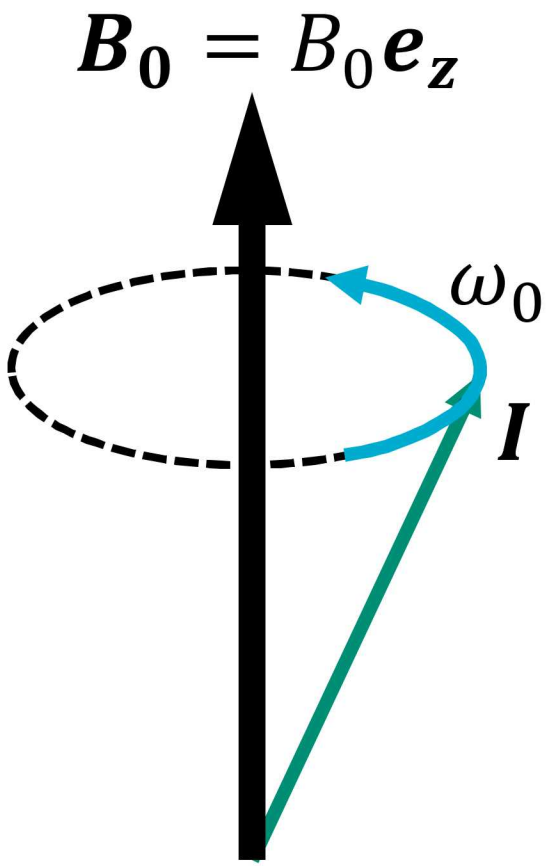

Right: Illustration of Larmor Precession in a static magnetic field

Optically Pumped Magnetometers(OPMs)

Atomic vapor is naturally in the maximally mixed state

$$\rho = \frac{1}{N}\mathbb{I}_N.$$

Where the Hilbert space of the atom has N total states and $\mathbb{I}_N$ is the $N \times N$ identity operator.

Before measuring precession, the state must be optically pumped into a metrologically useful state such as the "stretched state":

$$\rho = |F_a, m_F = F_a\rangle\langle F_a, m_F = F_a|.$$

Where $F_a = I + 1/2$ and

$F_b = I - 1/2$.

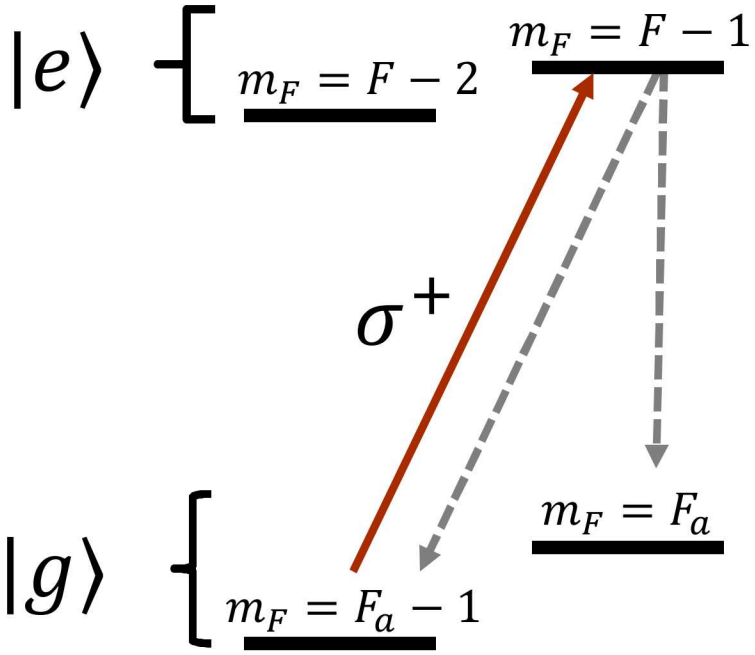

Above: Optical pumping with σ^+ polarized light causes population to accumulate in the "stretched" sate.

RF Magnetometry

Consider the effect an RF field transverse to $\boldsymbol{B_0}$:

$$\boldsymbol{B_{RF}}(t) = B_{RF}\sin(\omega_{RF}t)\,\boldsymbol{e_x}$$

Causes the state to rotate around $\boldsymbol{e_z}$ at frequency $2\omega_{RF}$ and oscillate between $\pm\boldsymbol{e_z}$ at frequency

$$\Omega' = \sqrt{(\Delta\omega)^2 + \Omega^2}.$$

Where $\Delta\omega = \omega_{RF} - \omega_0$ and

$$\Omega = \frac{1}{2}\gamma B_{RF}.$$

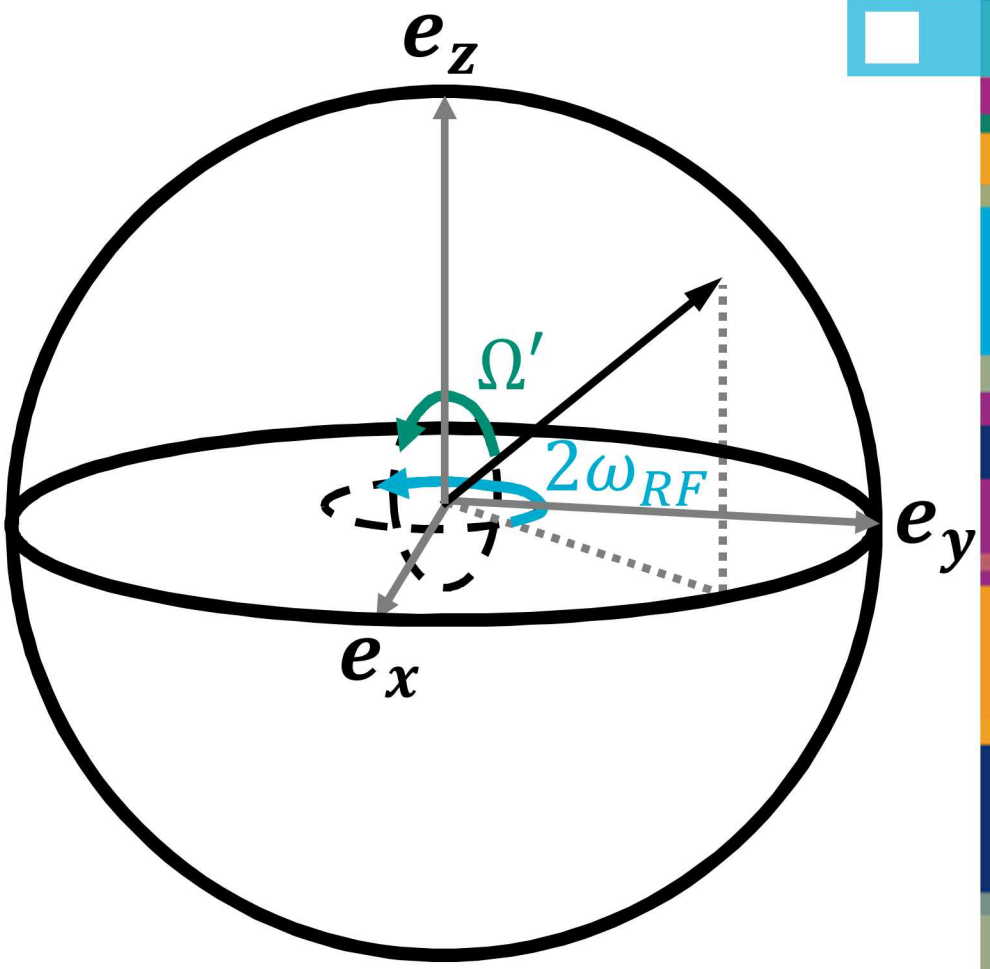

Above: Bloch sphere picture of the dynamics of the state in an RF magnetic field.

Practical RF Magnetometry

1. Pick frequency to measure f.
2. Tune B_0 so $f = 2\pi\omega_0$.
3. With $\Delta\omega \approx \omega_{RF}$, measure $\langle S_x(t)\rangle = \gamma B_{RF}[\alpha\cos(\omega_{RF}t) + \beta\sin(\omega_{RF}t)]$.

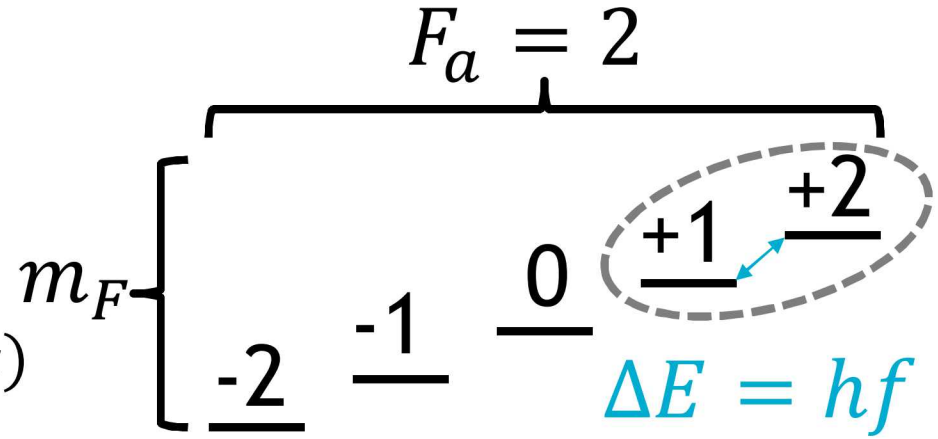

Right: Hyperfine ground state manifold of an $I = \frac{3}{2}$ alkali atom such as ^{87}Rb, with the Zeeman resonance of interest marked.

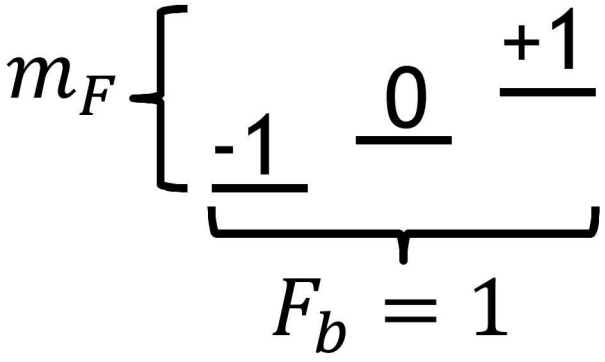

The Experimental Layout

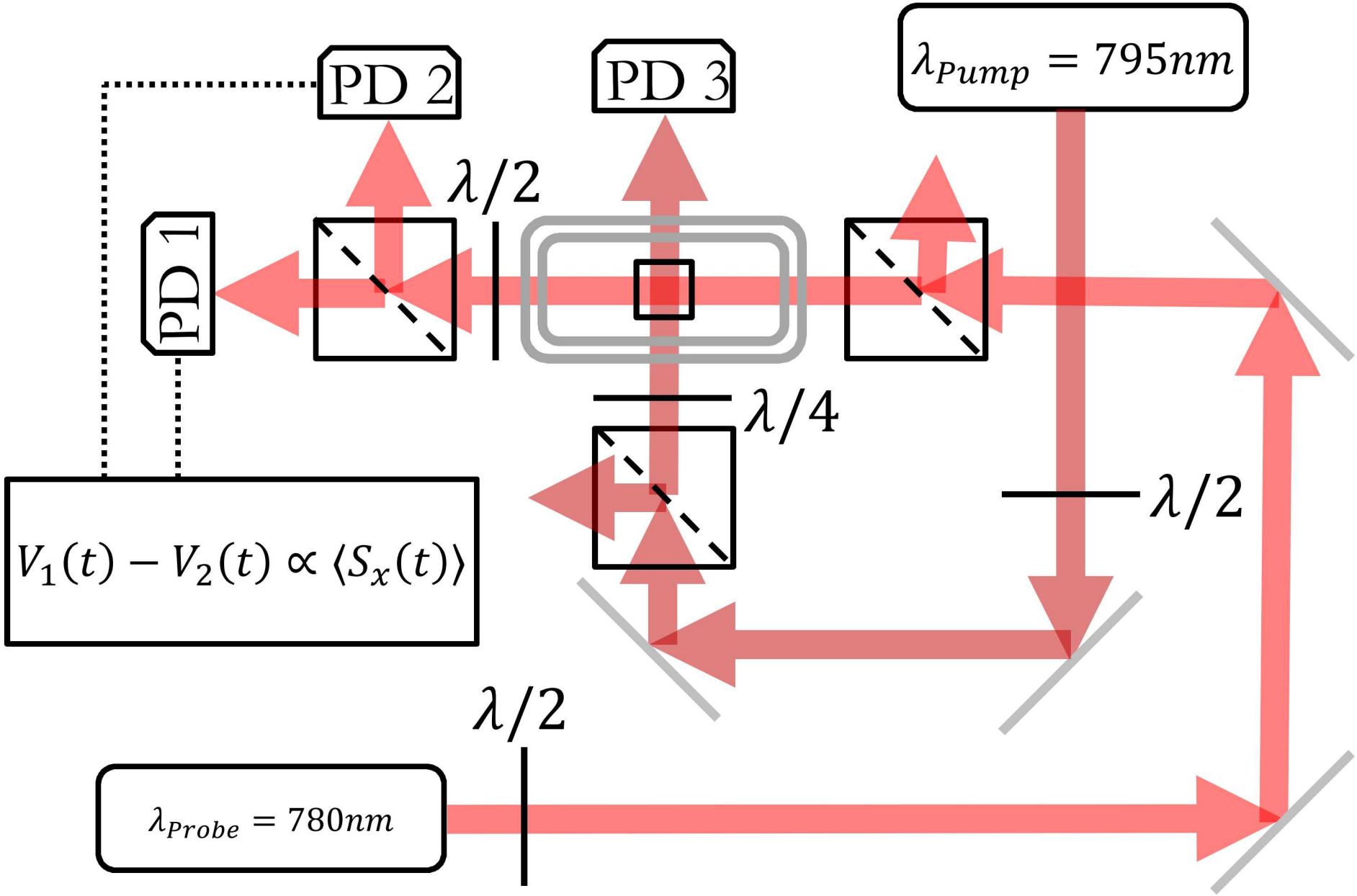

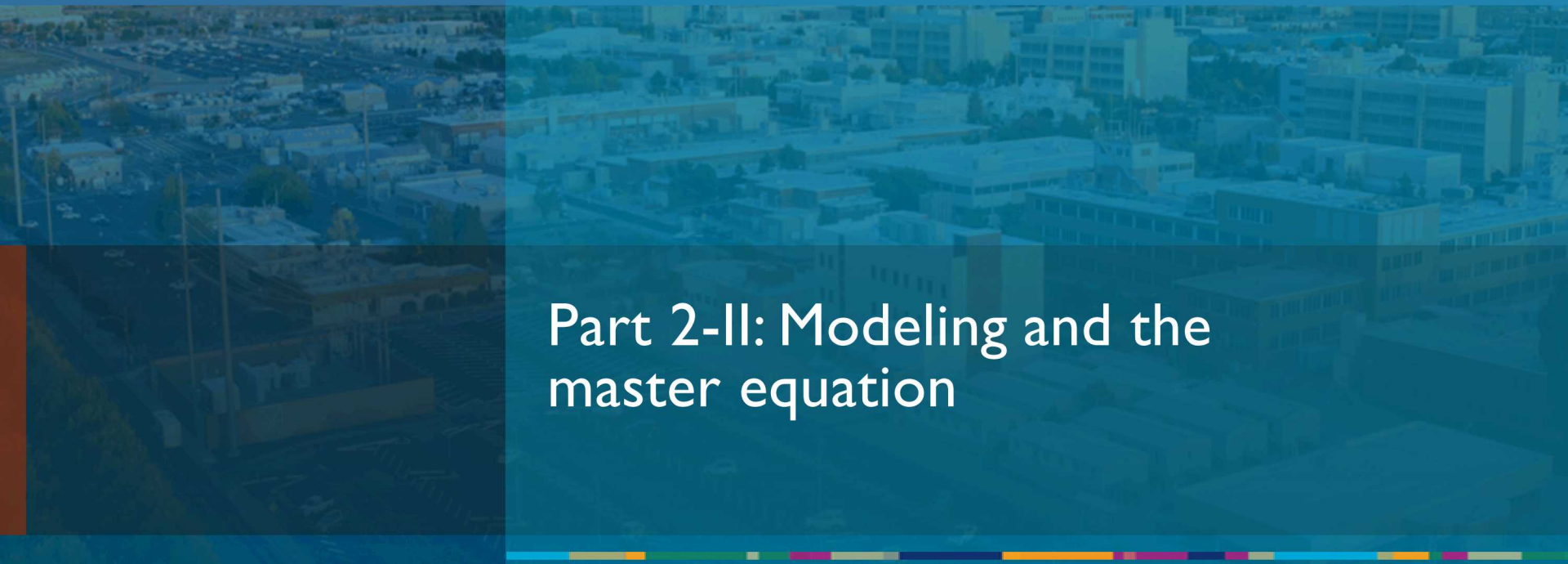

Part 2-II: Modeling and the master equation

The Master Equation

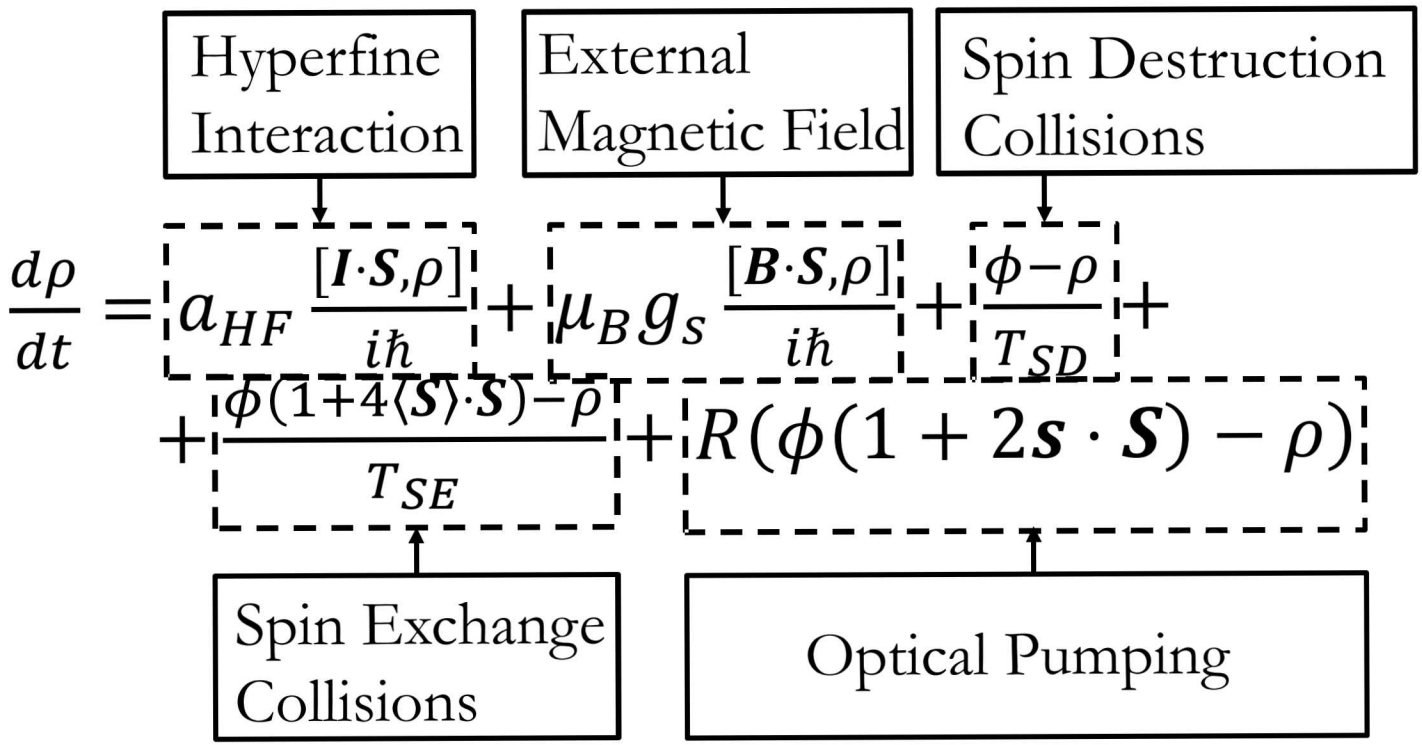

The Hyperfine Interaction

$$\left(\frac{d\rho}{dt}\right)_{Hyperfine} = a_{HF}[\boldsymbol{I}\cdot\boldsymbol{S},\rho]$$

This is the term from the free evolution of a single atom in vacuum.

- a_{HF} is the hyperfine coupling constant. It can be found in the literature.
- $\boldsymbol{I}$ is an $(N\times N)\times 3$ vector operator representing the nuclear spin of an atom.
- $\mathbf{S}$ is an $(N\times N)\times 3$ vector operator representing the electron spin of an atom.

Magnetic Field Coupling

$$\left(\frac{d\rho}{dt}\right)_{Mag} = \mu_B g_s \frac{[\boldsymbol{B}\cdot\boldsymbol{S},\rho]}{i\hbar}$$

- $\mu_B = 9.2740100783(28)\times 10^{-24}\frac{J^*}{T}$ is the Bohr Magneton.
- $g_s = 2.00231930436256(35)^*$ is the electron g-factor.
- $\hbar = \frac{1}{2\pi}6.62607015\times 10^{-34} J\cdot S^*$ is the reduced Plank's constant.
- $\boldsymbol{B} = B\boldsymbol{e_n}$ where B is a scaler in Teslas, and $\boldsymbol{e_n}$ is a 1×3 vector of unit length.

This term represents the interaction of the electron spin with an external magnetic field. The nuclear spin coupling is ~ 1000 times smaller, and can be neglected.

*CODATA values from NIST.

Spin Destroying Collisions

$$\left(\frac{d\rho}{dt}\right)_{SD} = \frac{\phi - \rho}{T_{SD}}$$

- $\phi = \rho/4 + \boldsymbol{S} \cdot \rho \boldsymbol{S}$ is the part of the density operator with only nuclear spin polarization $\Rightarrow \rho - \phi$ is the part with electron spin polarization.
- $R_{SD} = \frac{1}{T_{SD}} = \sum_j n_j \bar{v}_j \sigma_{SD,j}$ is the total spin destruction rate.
  - n_j is the denisty of the jth species with which the atoms are interacting
  - $\bar{v}_j$ is the average center of mass speed of the atoms relative to those of the jth species.
  - $\sigma_{SD,j}$ is the interaction cross section for spin−depolarizing collisions with the jth species.

This term represents the loss of coherence due to collisions that destroy the electron spin polarization.

Spin Exchanging Collisions

$$\left(\frac{d\rho}{dt}\right)_{SE} = \frac{\phi(1 + 4\langle \boldsymbol{S} \rangle \cdot \boldsymbol{S}) - \rho}{T_{SE}}$$

- $\frac{\phi - \rho}{T_{SE}}$ represents loss of coherence due to the collisions that exchange the spin between particles ($\boldsymbol{S}_1 \rightarrow \boldsymbol{S}_2$ & $\boldsymbol{S}_2 \rightarrow \boldsymbol{S}_1$).
- $\frac{4\phi\langle \boldsymbol{S} \rangle \cdot \boldsymbol{S}}{T_{SE}}$ gives the rate of redistribution of spin polarization from the spin exchange collisions, as the average spin $\langle \boldsymbol{S} \rangle = Tr(\rho \boldsymbol{S})$ of the ensemble interacts with spin of the individual electrons $\boldsymbol{S}$.
- $R_{SE} = \frac{1}{T_{SE}} = n\bar{v}\sigma_{SE}$ is the rate of spin exchange collisions, where n is the density, $\bar{v}$ is the average relative center of mass speed, and σ_{SE} is the interaction cross section for spin-exchanging collisions.

This complicated term describes how spin-exchanging collisions between alkali atoms both causes decoherence and redistributes spin polarization throughout the hyperfine manifold.

Optical Pumping

$$\left(\frac{d\rho}{dt}\right)_{OP} = R(\phi(1 + 2\boldsymbol{s}\cdot\boldsymbol{S}) - \rho)$$

- $R(\phi - \rho)$ represents loss of coherence due to the optical pumping field.
- $2R\phi\boldsymbol{s}\cdot\boldsymbol{S}$ represents the interaction of the average spin $\boldsymbol{s} = s\boldsymbol{e_n}$ of the photons in the pumping field with the spin $\boldsymbol{S}$ of the electron(s).

This term represents the interaction of the atom(s) with the light field used for optical pumping.

Setting up the Calculation

- All operators can be represented as $N \times N$ matrices, where $N = 2(2I + 1)$.
- Angular momentum operators $\boldsymbol{F}, \boldsymbol{I}, \boldsymbol{S}$ can be found in spherical basis.
  - $\boldsymbol{e}_{\pm 1} = \mp \frac{1}{\sqrt{2}} \boldsymbol{e}_{\boldsymbol{x}} - \frac{i}{\sqrt{2}} \boldsymbol{e}_{\boldsymbol{y}}$, $\boldsymbol{e}_{\boldsymbol{0}} = \boldsymbol{e}_{\boldsymbol{z}}$
  - Find $\langle F, m_F | \boldsymbol{J} | F', m_{F'} \rangle$ for convenient values of F, m_F using ladder operators, where $\boldsymbol{J} = \boldsymbol{F}, \boldsymbol{S}$.
  - From Wigner-Eckart theorem:

$$\langle F, m_F \left| \boldsymbol{J}_q \right| F', m_{F'} \rangle = \langle F', m_{F'}, 1, q | F, m\_F \rangle \langle F \left|\left| \boldsymbol{J} \right|\right| F' \rangle.$$

Where $q = \pm 1, 0$ is the spherical index. The first term on the right is a Clebsh-Gordan coefficient, and the second is a reduced matrix element.

- With operators in hand, calculate $\frac{d\rho}{dt}$ for a given input state ρ

MATLAB Implementation: The Basis Representation

The basis is illustrated below for $I = \frac{3}{2}$. m_F values are in ascending order, so $\rho_{11} = |F_b, m_F = -F_b\rangle\langle F_b, m_F = -F_b|$, $\rho_{22} = |F_b, m_F = -F_b + 1\rangle\langle F_b, m_F = -F_b + 1|$ etc. After the lower hyperfine manifold, it restarts at the bottom of the upper manifold, so $\rho_{44} = |F_a, m_F = -F_a\rangle\langle F_a, m_F = -F_a|$, etc.

$F = F_b = 1$

$$\rho = \begin{bmatrix} \rho_{11} & \rho_{12} & \rho_{13} & \rho_{14} & \rho_{15} & \rho_{16} & \rho_{17} & \rho_{18} \\ \rho_{21} & \rho_{22} & \rho_{23} & \rho_{24} & \rho_{25} & \rho_{26} & \rho_{27} & \rho_{28} \\ \rho_{31} & \rho_{32} & \rho_{33} & \rho_{34} & \rho_{35} & \rho_{36} & \rho_{37} & \rho_{38} \\ \rho_{41} & \rho_{42} & \rho_{43} & \rho_{44} & \rho_{45} & \rho_{46} & \rho_{47} & \rho_{48} \\ \rho_{51} & \rho_{52} & \rho_{53} & \rho_{54} & \rho_{55} & \rho_{56} & \rho_{57} & \rho_{58} \\ \rho_{61} & \rho_{62} & \rho_{63} & \rho_{64} & \rho_{65} & \rho_{66} & \rho_{67} & \rho_{68} \\ \rho_{71} & \rho_{72} & \rho_{73} & \rho_{74} & \rho_{75} & \rho_{76} & \rho_{77} & \rho_{78} \\ \rho_{81} & \rho_{82} & \rho_{83} & \rho_{84} & \rho_{85} & \rho_{86} & \rho_{87} & \rho_{88} \end{bmatrix}$$

$F = F_a = 2$

MATLAB Implementation: Simulation Procedure

1. A set of functions calculates $a_{HF}, 1/T_{SE}, 1/T_{SD}$ at a given temperature from literature values for given species.
2. Another function calculates $\boldsymbol{F}, \boldsymbol{I}, \boldsymbol{S}$ from the value of I for the alkali in question.
3. A third function takes these along with an input state ρ, an external magnetic field $\boldsymbol{B}$, and the mean photon polarization vector $\boldsymbol{s}$ to compute the evolution $\frac{d\rho}{dt}$.
4. An initial state ρ_0, mean photon polarization $\boldsymbol{s}$, and magnetic field $\boldsymbol{B}$(t) are chosen and used with the evolution function to feed into built in ODE solver.
   - Solutions are "stiff", requiring use of correct ODE solver.
5. Out comes $\rho(t)$!

Part 2-III:Results

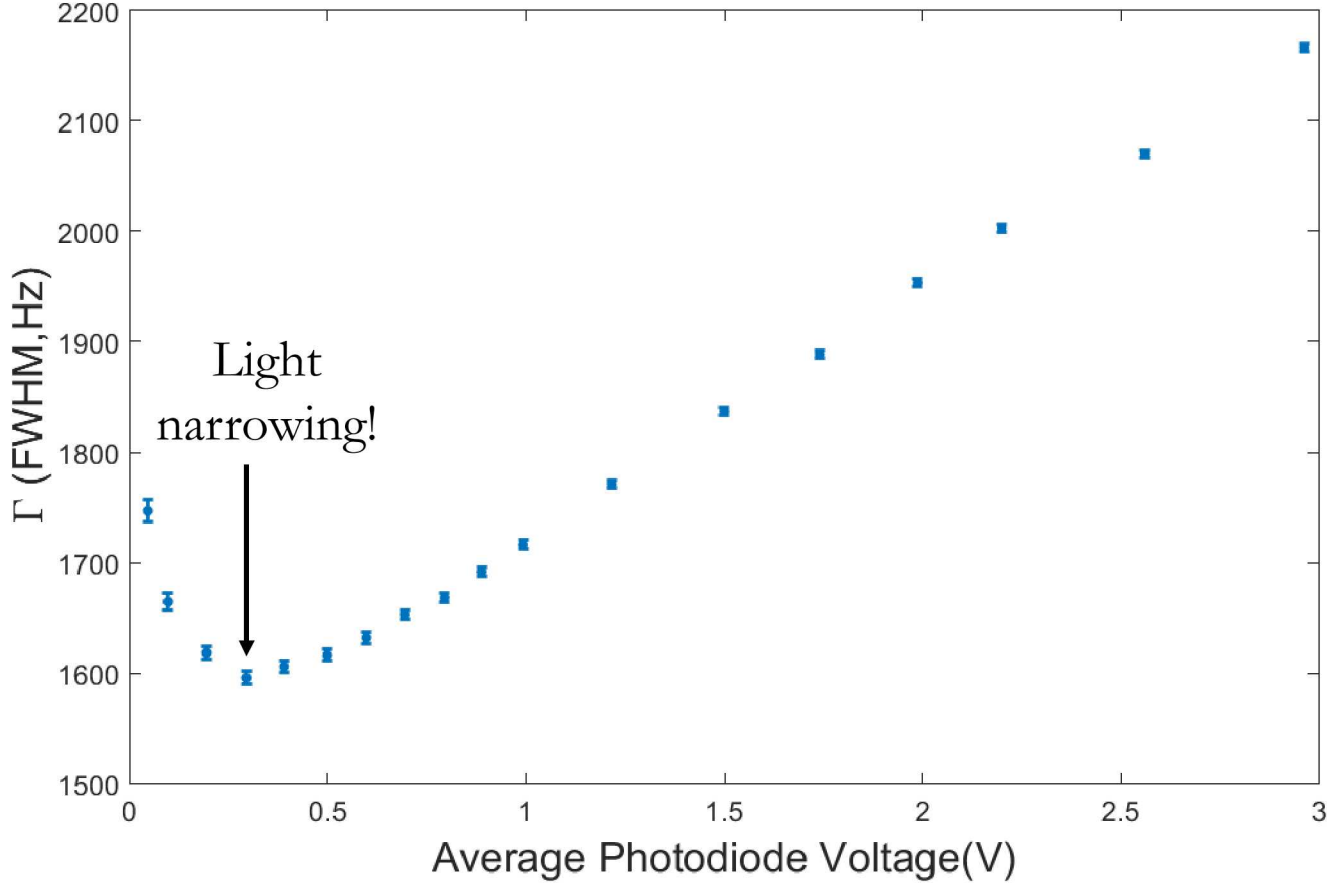

Above: Data showing the dependence of the Zeeman resonance linewidth Γ on the power of the optical pumping beam. Error bars are 95% confidence bounds of Lorentzian fit. The resonance frequency was $f_0 = 2\pi\omega_0 \approx 24.125kHz$ for these measurements.

Extraction of the Pumping Rate

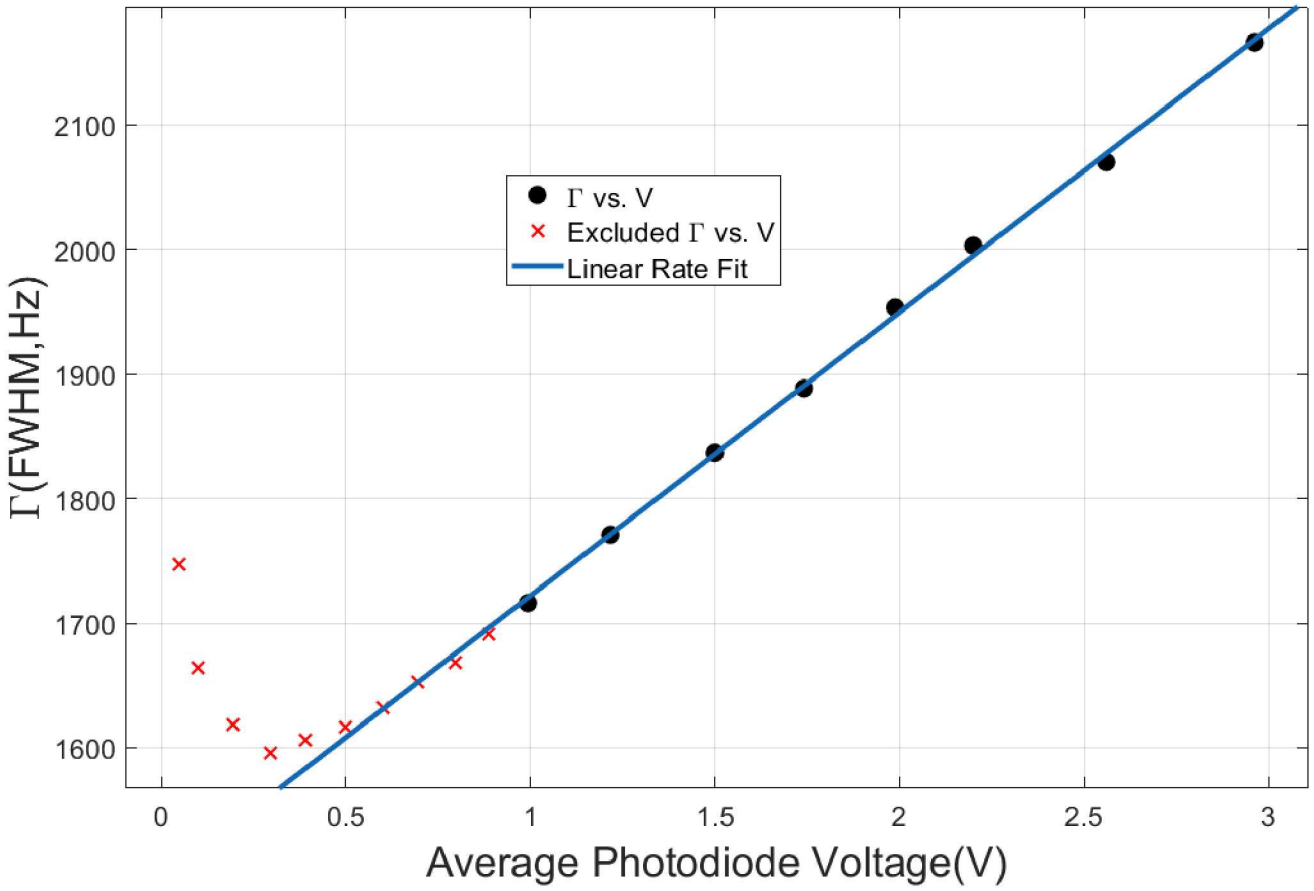

Above: Liner fit to the equation $\Gamma \approx \frac{R_{OP}}{4}$+b for $\frac{R_{SD}R_{SE}}{R_{OP}^2} \ll 1$.(1) A fit to $\Gamma = \frac{aV}{4} + \mathrm{b}$ thus gives $R_{OP} = aV$. This fit gives $a = 910.2(879.5,940.8)s^{-1}/V$.

(1) Analytic form from the Savukov, Seltzer, and Romalis "Tunable Atomic Magnetometer for Detection of Radio-Frequency Magnetic Fields", PRL 95, 063004(2005). I have added the offset term "b".

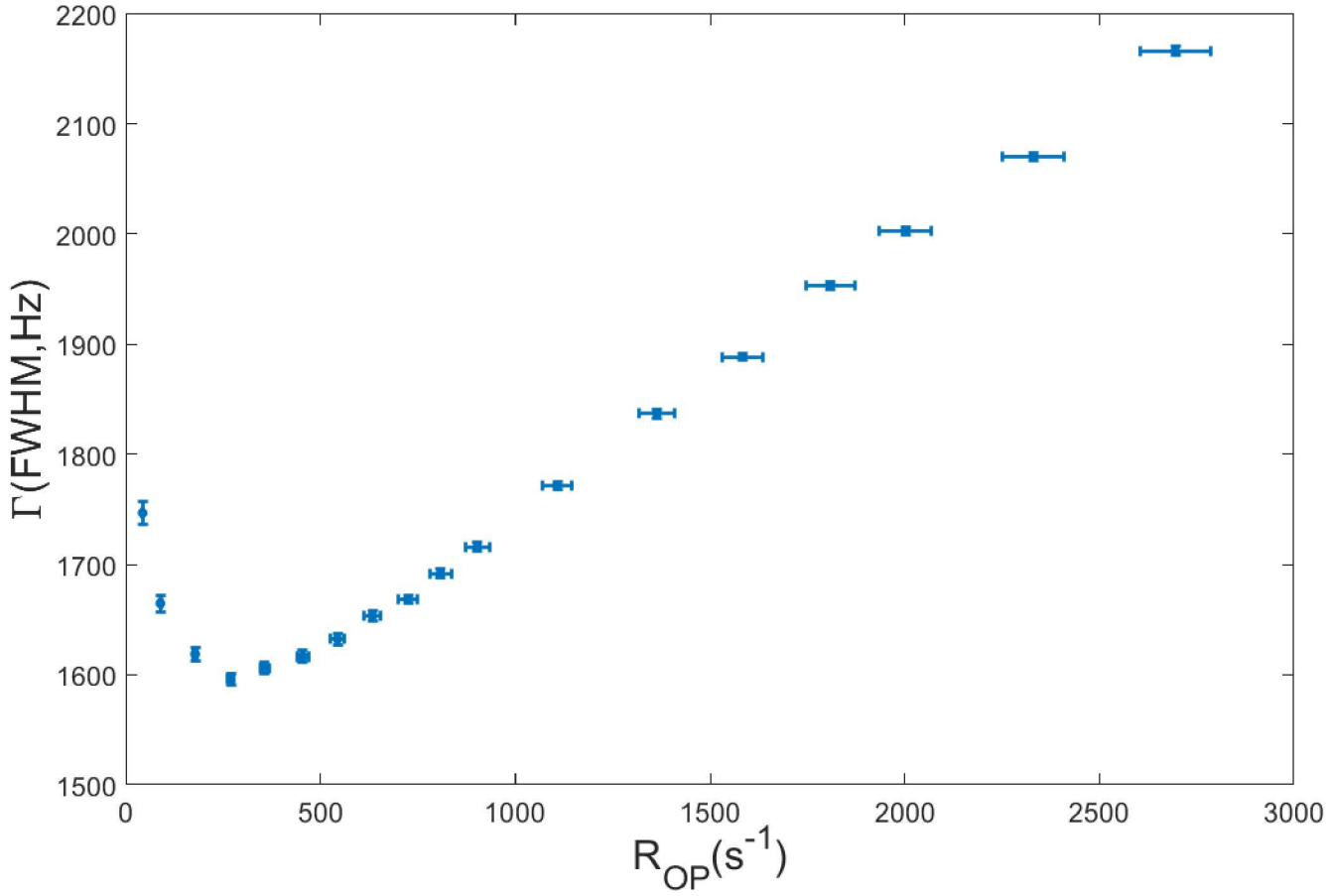

Above: The linewidth as a function of optical pumping rate with error bars given by 95% confidence intervals of the linear fit.

Comparison with Theory

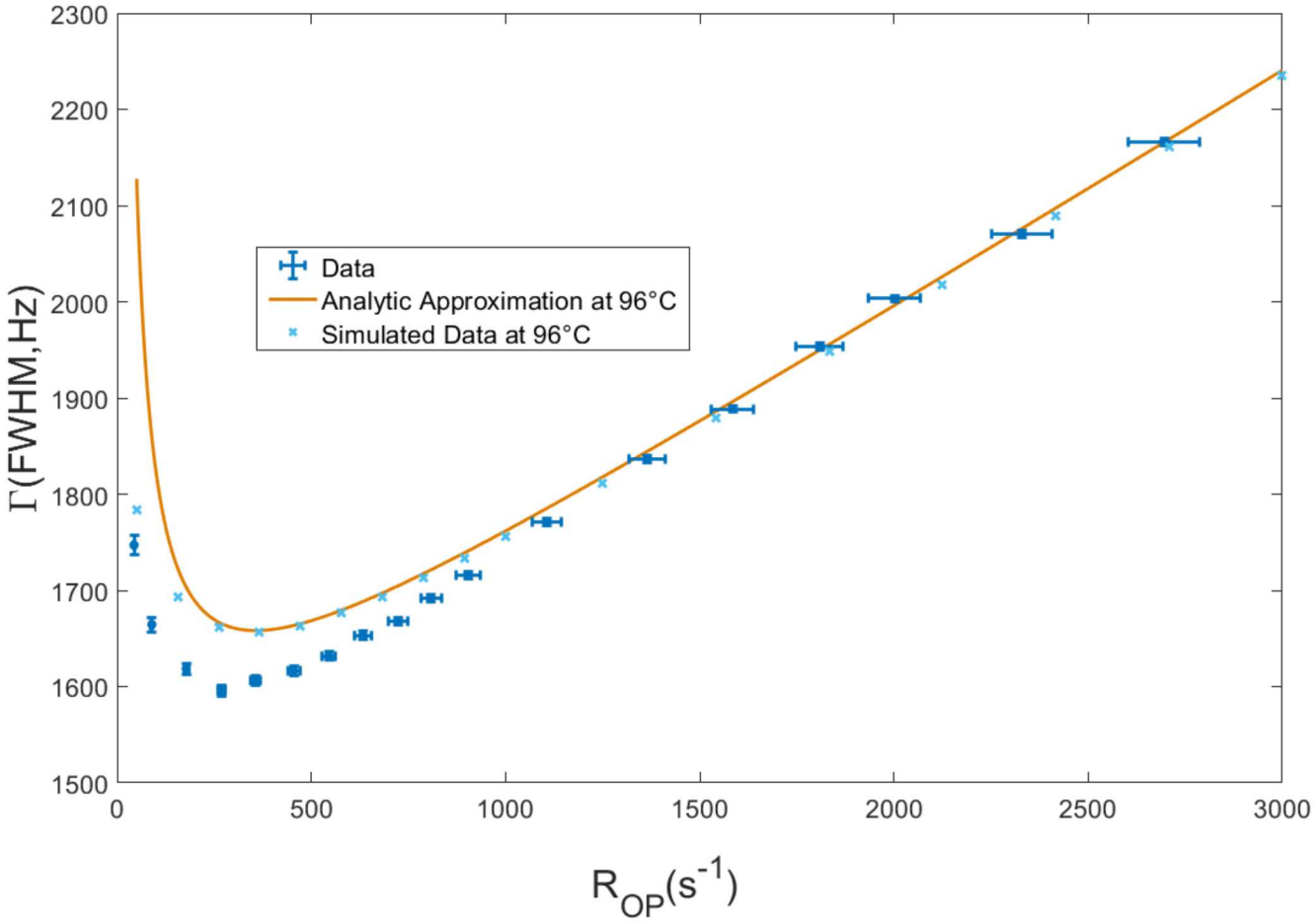

Above: Comparison of data to the analytic approximation $\Gamma \approx \frac{R_{OP}}{4} + \frac{R_{SE}R_{SD}}{5R_{OP}} + \mathrm{b}$ where R_{SE} and R_{SD} were computed for the temperature $T = 96^{\circ}C$ as measured from our thermocouple. The result from a fit based on numerical simulations of the density matrix is also included.

Part II-IV-Future Work

Short Term (By the end of the Semester)

1. Install third coil pair for three axis magnetic field control
   - Will allow for the field to be fully zeroed.
2. Analyze optical linewidth data to extract the density of buffer gas n_{N_2}.
3. Investigate in the low magnetic field "spin exchange relaxation free"(SERF) regime to extract the spin destruction and exchange rates, along with an independent calibration of the optical pumping rate.
4. Investigate the effect of RF power broadening on the Zeeman resonance linewidth.
5. Add a heatsink to OP-AMP to reach higher temperatures.

Medium Term(By the end of the year)

1. Characterize the sensitivity/noise floor of our magnetometer from DC to 300kHz.
2. Try several cells with different isotopic combinations (natural abundance Rb, 133Cs?) and buffer gas pressures.
   - Expand simulation framework for multiple alkali isotopes by taking
     $$\rho = a\rho_1 + b\rho_2.$$
   - Ensure that the simulation agrees well under multiple configurations. If not, figure out why and adjust.
3. Decide on a final alkali species and buffer gas combination for our needs.

Long Term (By the end of the Project, 2022)

1. Build an active feedback coil system to work without shielding.
   - Use an FPGA for fast logic?
   - Use Labview?
   - Hybrid system (atoms+classical) for rough zeroing?
2. Design a compact mobile palatiform.
   - Minimize size and power consumption.
3. Try to see if we can pick up real signals outdoors with it!

Part III: Acknowledgements

The Rydberg Project

- Thanks to Sandia National Laboratories for providing funding for through the ΣIGMA grand challenge, along with pervious funding through a number of other laboratory programs.
- Thanks to CQuIC for providing me with this amazing research opportunity.
  - Special thanks to professor Deutsch and his quantum optics course .
  - Thanks also to Adrian Orozco and Nate Ristoff.
- Thanks to everyone at UNM and Sandia who have contributed to the Rybderg Project.
  - Special thanks to my advisor, Grant Biedermann.
  - Special thanks also to Prof. Alberto Marino and Mike Martin.

Above: Prof. Grant Biedermann

Below: Mike Martin

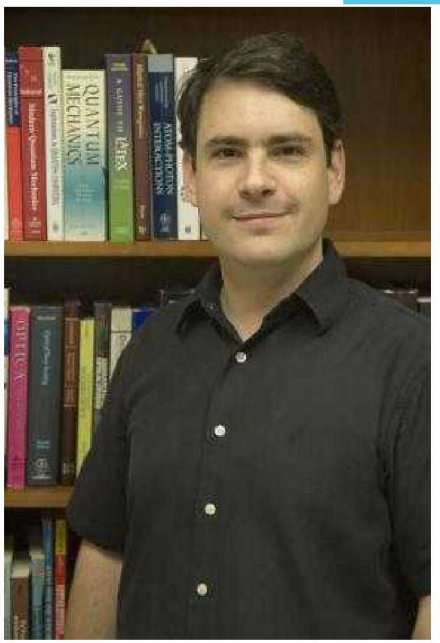

Above: Prof. Alberto Marino

Below: Prof. Ivan Deutsch

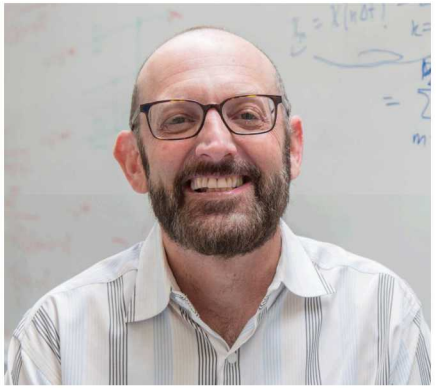

The RF Magnetometer

- Thanks to Sandia National Labs for providing funding through the laboratory directed research and development (LDRD) program for this work.
- Thanks to Peter Schwindt for giving me the opportunity to work on this project, and his continuing mentorship.
- Thanks to Neil Claussen for his ongoing help with all aspects of the project.

Above: Peter Schwindt

Below: Neil Claussen